Electronic Supplementary Information

Unprecedented Infinite Lanthanide Hydroxide Ribbons $[Ln_3(\mu_3\text{-}OH)_3]_n^{6n+}$ in 3-D Metal-organic Framework

Rui-Li Sang and Li Xu*

State Key Laboratory of Structural Chemistry, Fujian Institute of Research on the Structure of Matter, Chinese Academy of Science, Fuzhou, Fujian, 350002, China

E-mail: xli@fjirsm.ac.cn

Experimental Section

Materials and methods

All commercially available chemicals are of reagent grade and used as supplied without further purification. 1, 1'-di(ethylpropionato)-2, 2'-biimidazole ($Epra_2biim$) was synthesized in accordance with a published procedure.[1] H_2Pra_2biim was prepared by hydrolyzing $Epra_2biim$ and characterized by IR spectra and ^1H NMR. The C, H and N microanalyses were carried out with a Vario EL III elemental analyzer. Infrared spectra were recorded on a Magna 750 FT-IR spectrometer photometer as KBr pellets in the 4000-400cm^{-1}. TGA were recorded with a Netzsch STA449C-QMS 403 C apparatus under a nitrogen atmosphere. All of magnetic measurements were performed using a commercial Quantum Design Physical Property Measurement System (PPMS-9T) and Magnetic Property Measurement System (MPMS(SQUID)-XL).

Synthesis of $[Ln_3(\mu_3\text{-}OH)_3(Pra_2biim)_3(H_2O)]_n \cdot 4nH_2O$ [Ln = Nd(1), Pr(2) and La(3)].

A mixture of $Ln(NO_3)_2 \bullet 6H_2O$ (0.033 mmol; $Nd(NO_3)_3 \cdot 6H_2O$, 0.0146 g;

$Pr(NO_3)_3·6H_2O$, 0.0145 g; $La(NO_3)_2·6H_2O$, 0.0143 g), H_2Pra_2biim (0.05 mmol, 0.0139 g) and NaOH (0.14mmol, 0.0056g) in H_2O (3 mL) were sealed in a 20 mL Teflon-lined stainless steel autoclave. The autoclave was heated at 130 ℃ for 3 days under autogenous pressure. After cooling, crystals of **1-3** were obtained. For **1**: Yield: 47% (based $Nd(NO_3)_3·6H_2O$). Anal. Calcd. for $C_{36}H_{51}N_{12}Nd_3O_{21}$ (Mr = 1420.58): C 30.44; H 3.62; N 11.83; Found: C 30.01; H 3.66; N 11.77%. IR (KBr, cm^{-1}): 3735m, 3650m, 3673m, 3631m, 3568m, 1682m, 1596m, 1542vs, 1500vs, 1508m, 1475m, 1439s, 1420vs, 1377m, 1278m, 1240m, 1184m, 1130m, 1105w, 1029w, 949w, 891w, 758m, 738m, 713m, 669m, 496w. For **2**: Yield: 52% (based $Pr(NO_3)_3·6H_2O$). Anal. Calcd. for $C_{36}H_{51}N_{12}Pr_3O_{21}$ (Mr = 1410.58): C 30.65; H 3.64; N 11.92; Found: C 30.70; H 3.76; N 12.18%. IR (KBr, cm^{-1}): 3734m, 3650m, 3631m, 3616m, 3589m, 1682m, 1650m, 1596m, 1542vs, 1508m, 1508m, 1475m, 1459m, 1440s, 1424vs, 1376m, 1279m, 1240m, 1184m, 1130m, 1105w, 1030w, 948w, 890w, 738m, 713m, 669m, 491w. For **3**: Yield: 49% (based $La(NO_3)_3·6H_2O$). Anal. Calcd. for $C_{36}H_{51}La_3N_{12}O_{21}$ (Mr = 1404.57): C 30.78; H 3.66; N 11.97; Found: C 28.95; H 3.64; N 11.09%. IR (KBr, cm^{-1}): 3595m, 3363m, 3140m, 3110m, 1635m, 1590s, 1546vs, 1462m, 1440s, 1425vs, 1339w, 1280m, 1250w, 1131w, 1106w, 1042w, 1031w, 946w, 919m, 757m, 738m, 726m, 713m, 668m, 635w. 496w.

X-Ray crystallography

The intensity data were collected on a Mercury CCD diffractometer for **1** and **2**, and Saturn724 CCD diffractometer for **3** with graphite-monochromated MoKα radiation (λ = 0.71073 Å). All absorption corrections were performed by using the multiscan program. The structure were solved by direct methods and refined by full-matrix least squares on F^2 with the SHELXTL-97 program.[2] The only C11 atom of the Pra_2biim^{2-} ligand is disordered to two positions (C11A/C11B) in compounds **1-3**. Thermal (SIMU and DELU) restraints are placed on Atoms C11A, C11B and C10 in **1** and **2**. Thermal (SIMU and DELU) restraints are placed on atoms C11A, C11B and C10, and bond (DFIX and SADI) restraints are applied to these bonds (C11a-C10, C11b-C10,

C11a-C12 and C11b-C10) in **3**. The 3.5 guest water molecules were crystallographically well defined in **1**, **2** and **3**, and the number of isolated water molecules was 4 determined on the basis of TGA and elemental microanalyses. Crystal data as well as details of data collection and refinement for the complexes are summarized in Table 1S. The hydrogen bonding parameters are shown in Table 2S-4S. Table 5S show comparison of the conformation of Pra_2biim^{2-} of complexe **1**. CCDC-923601 (**1**), CCDC-923602 (**2**), and CCDC-923600 (**3**) contain the supplementary crystallographic data for this paper, these data can be obtained free of charge from the Cambridge Crystallographic Data Centre via www.ccdc.cam.ac.uk/data_request/cif.

Table 1S Crystallographic data for compounds **1-3.**

Complex	**1**	**2**	**3**
Molecular formula	$C_{36}H_{50}N_{12}Nd_3O_{20.50}$	$C_{36}H_{50}N_{12}O_{20.50}Pr_3$	$C_{36}H_{50}La_3N_{12}O_{20.50}$
Formula weight	1411.60	1401.61	1395.61
Crystal system	Orthorhombic	Orthorhombic	Orthorhombic
Space group	$P2_12_12_1$	$P2_12_12_1$	$P2_12_12_1$
a (Å)	10.701(2)	10.732(2)	10.874(4)
b (Å)	18.247(4)	18.271(4)	18.405(8)
c (Å)	25.046(6)	25.052(6)	25.171(11)
Volume ($Å^3$)	4890.9(18)	4912.0(18)	5038(4)
Z	4	4	4
d_{calc} (g/cm_3)	1.917	1.895	1.840
μ (mm^{-1})	3.226	3.017	2.584
F(000)	2776	2764	2740
Reflns Collected	38143	38454	42821
Unique reflns	11184	11208	11400
Completeness to θ	99.9 %	99.7 %	99.7 %
Refined parameters	659	659	660
flack	-0.003(9)	-0.004(11)	0.03(3)
Goodness of fit	1.100	1.107	1.150
$R_1{}^a/\omega R_2{}^b$ [$I > 2\sigma(I)$]	0.0257, 0.0508	0.0295, 0.0581	0.0708, 0.1618
$R_1{}^a/\omega R_2{}^b$ (all data)	0.0269, 0.0518	0.0313, 0.0594	0.0770, 0.1700

$^aR_1 = \Sigma||Fo|-|Fc|| / \Sigma|Fo|$. $^bwR_2 = \{\Sigma[w(F_o^2-F_c^2)^2]/ \Sigma[w(F_o^2)^2]\}^{1/2}$.

Table 2S Hydrogen Bonds for compound **1.**

D–H…A	d(D-H) (Å)	d(H...A) (Å)	d(D...A) (Å)	∠(DHA) (°)
O(1)-H(1A)...O(1W)#2	0.82	2.33	3.124(5)	163.1
O(2)-H(2A)...O(1W)	0.82	2.31	3.107(5)	166.6
O(3)-H(3A)...O(2W)	0.85	2.34	3.167(6)	164.7

O(4)-H(4C)...O(2W)	0.85	1.88	2.723(6)	176.9
O(4)-H(4D)...N(6)#1	0.85	2.13	2.939(5)	159.6
O(5)-H(5C)...N(2)#3	0.84	2.14	2.889(5)	148.1
O(5)-H(5D)...O(8)#3	0.85	2.02	2.868(5)	176.0
O(1W)-H(1WB)...O(10)	0.95	2.34	2.971(6)	123.1
O(1W)-H(1WA)...O(3W)#5	0.89	2.32	2.998(6)	132.4
O(2W)-H(2WA)...O(11)	0.79	1.98	2.730(5)	157.2
O(2W)-H(2WB)...O(3W)	0.78	2.18	2.890(7)	150.8
O(3W)-H(3WA)...N(2)#4	0.83	2.53	3.347(6)	168.9
O(3W)-H(3WA)...O(5)#2	0.83	2.64	3.167(5)	122.8
O(3W)-H(3WB)...N(8)#6	0.85	1.96	2.802(6)	170.6
O(4W)-H(4WA)...N(12)	0.86	2.33	3.138(15)	154.9
O(4W)-H(4WB)...O(15)	0.87	2.15	3.011(13)	179.5

Symmetry code: #1 -x+1,y+1/2,-z+1/2; #2 x-1/2,-y+1/2,-z+1; #3 -x+3/2,-y+1,z+1/2; #4 -x+1,y-1/2,-z+1/2; #5 x+1,y,z; #6 x-1,y,z.

Table 3S Hydrogen Bonds for compound **2**.

D–H…A	d(D-H) (Å)	d(H...A) (Å)	d(D...A) (Å)	∠(DHA) (°)
O(1)-H(1A)...O(1W)#2	0.82	2.34	3.133(6)	163.1
O(2)-H(2A)...O(1W)	0.82	2.30	3.099(6)	166.9
O(3)-H(3A)...O(2W)	0.84	2.34	3.159(6)	165.3
O(4)-H(4C)...O(2W)	0.84	1.89	2.732(6)	177.2
O(4)-H(4D)...N(6)#1	0.83	2.14	2.933(6)	158.9
O(5)-H(5C)...N(2)#3	0.84	2.14	2.878(5)	147.3
O(5)-H(5D)...O(8)#3	0.84	2.01	2.854(5)	177.2
O(1W)-H(1WA)...O(3W)#5	0.90	2.31	2.990(7)	131.9
O(1W)-H(1WB)...O(10)	0.94	2.36	2.968(7)	122.2
O(2W)-H(2WA)...O(11)	0.79	1.98	2.738(6)	159.0
O(2W)-H(2WB)...O(3W)	0.76	2.20	2.877(8)	149.4
O(3W)-H(3WA)...N(2)#4	0.83	2.53	3.354(7)	169.7
O(3W)-H(3WA)...O(5)#2	0.83	2.63	3.150(6)	122.0
O(3W)-H(3WB)...N(8)#6	0.86	1.96	2.811(7)	171.9
O(4W)-H(4WA)...N(12)	0.86	2.36	3.154(19)	154.6
O(4W)-H(4WB)...O(15)	0.87	2.13	2.998(17)	178.4

Symmetry code: #1 -x+1,y+1/2,-z+1/2; #2 x-1/2,-y+1/2,-z+1; #3 -x+3/2,-y+1,z+1/2; #4 -x+1,y-1/2,-z+1/2; #5 x+1,y,z; #6 x-1,y,z.

Table 4S Hydrogen Bonds for compound **3**.

D–H…A	d(D-H) (Å)	d(H...A) (Å)	d(D...A) (Å)	∠(DHA) (°)
O(1)-H(1C)...O(2W)#2	0.84	2.45	3.231(15)	156.2
O(2)-H(2C)...O(2W)	0.84	2.35	3.149(15)	159.3
O(2)-H(2C)...O(10)	0.84	2.51	3.047(11)	122.4
O(3)-H(3C)...O(1W)#7	0.84	2.36	3.192(15)	171.0
O(4)-H(4C)...N(6)#1	0.90	2.02	2.870(15)	157.1
O(4)-H(4D)...O(1W)#7	0.85	1.90	2.745(16)	179.1

O(5)-H(5C)...O(8)#3	0.92	2.15	2.843(14)	131.6
O(5)-H(5C)...O(14)	0.92	2.40	3.025(13)	124.8
O(5)-H(5D)...N(2)#3	0.91	2.03	2.842(13)	148.5
O(1W)-H(1WA)...O(11)#8	0.88	2.02	2.768(15)	143.0
O(1W)-H(1WA)...O(3)#8	0.88	2.65	3.192(15)	121.4
O(1W)-H(1WB)...O(3W)#9	0.85	2.07	2.92(2)	179.3
O(2W)-H(2WB)...O(10)	0.93	2.36	2.990(17)	124.8
O(2W)-H(2WA)...O(12)#5	0.85	2.28	3.134(16)	179.4
O(3W)-H(3WA)...N(2)#6	0.88	2.47	3.346(18)	171.6
O(3W)-H(3WB)...O(2W)#10	0.97	2.14	2.991(19)	145.5
O(4W)-H(4WA)...O(15)#6	0.85	2.04	2.89(7)	175.2
O(4W)-H(4WB)...N(10)#4	0.87	1.85	2.61(6)	144.0

Symmetry code: #1 -x+2,y-1/2,-z+1/2 ; #2 x+1/2,-y+1/2,-z; #3 -x+3/2,-y,z-1/2; #4 -x+1, y+1/2,-z+1/2; #5 -x+1,y-1/2,-z+1/2; #6 -x+3/2,-y,z+1/2; #7 x+1,y,z; #8 x-1,y,z; #9 x-1/2, -y+1/2,-z+1; #10 x+1/2,-y+1/2,-z+1

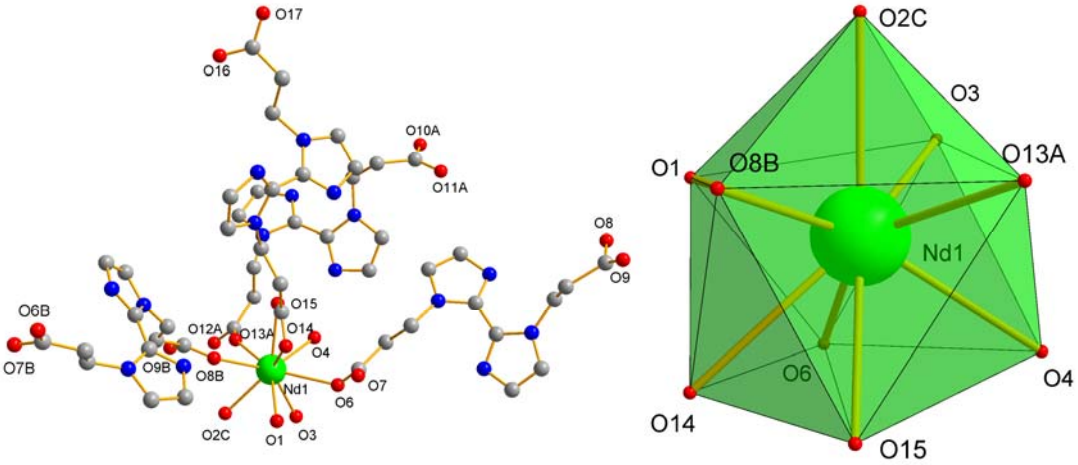

(a)

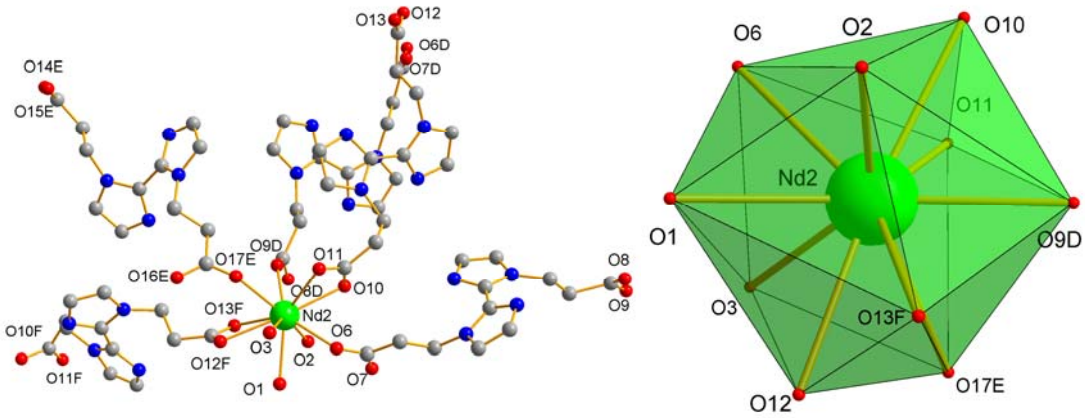

(b)

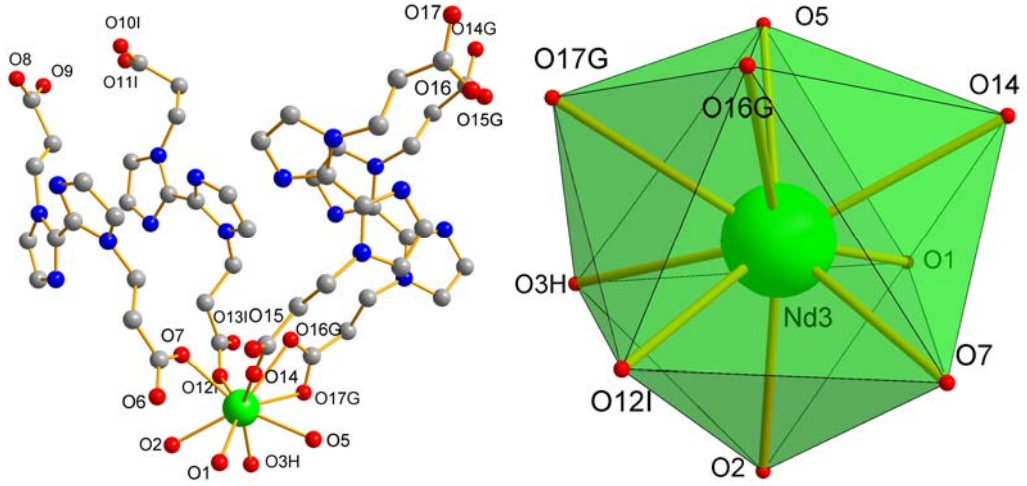

(c)

Fig. 1S The coordination environments and the polyhedral representation of Nd1 (a), Nd2 (b) and Nd3 (c) atoms in **1**. Symmetry code: A: 1-x, 0.5+y, 0.5-z; B: 1.5-x, 1-y, 0.5+z; C: -0.5+x, 0.5-y, 1-z; D: 2-x, -0.5+y, 0.5-z; E: x, -1+y, z; F: 1.5-x, -y, 0.5+z; G: 0.5+x, 1.5-y, 1-z; H: 0.5+x, 0.5-y, 1-z; I: 2-x, 0.5+y, 0.5-z.

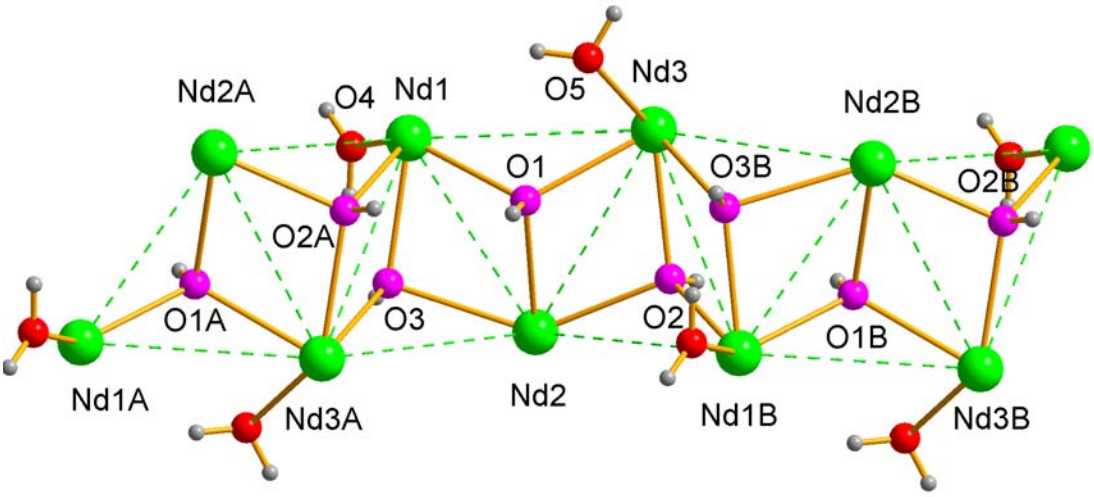

Fig. 2S $[Nd_3(\mu_3\text{-}OH)_3(H_2O)_2]_n^{6n+}$ ribbon-like chain in **1**. Symmetry code: A: -0.5+x, 0.5-y, 1-z; B: 0.5+x, 0.5-y, 1-z.

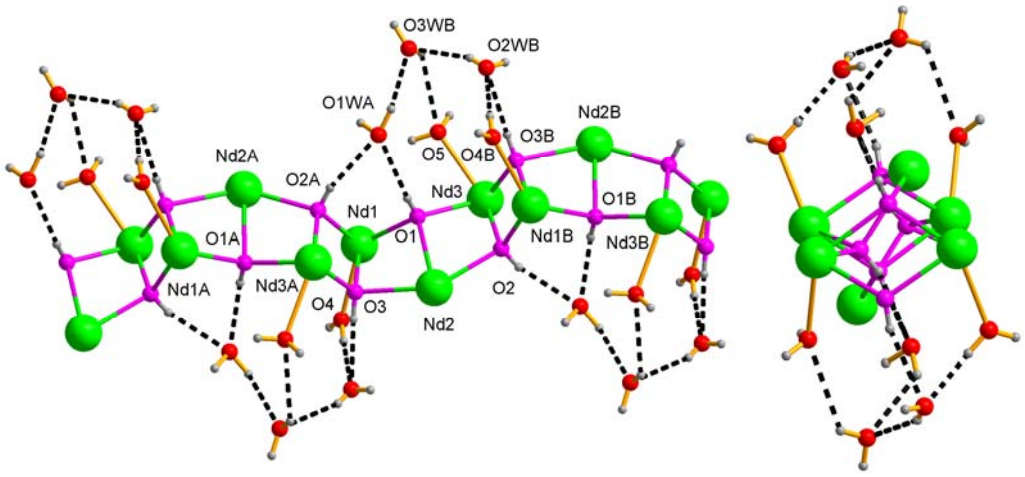

Fig. 3S H-bonds (black dashed lines) between the $[Nd_3(\mu_3\text{-}OH)_3(H_2O)_2]_n^{6n+}$ ribbon-like chain and the lattice water molecules along different direction. Symmetry code: A: -0.5+x, 0.5-y, 1-z; B: 0.5+x, 0.5-y, 1-z.

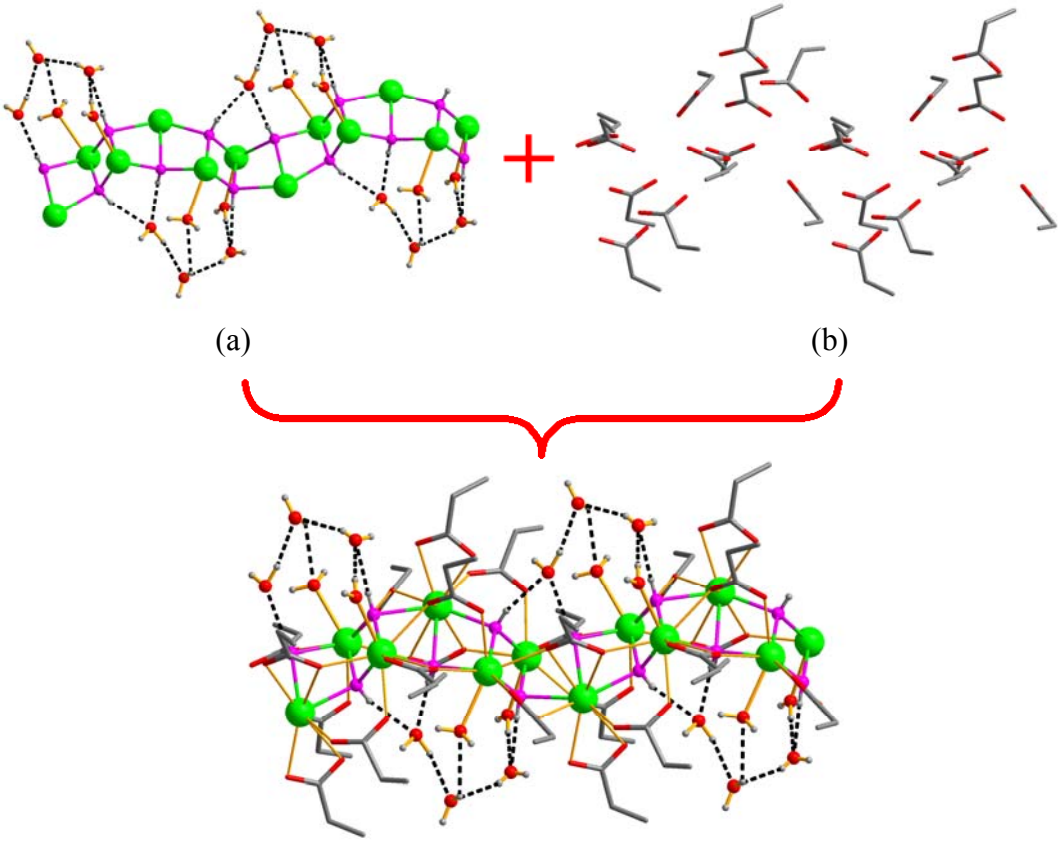

Fig. 4S View of the lattice water molecules located in the cavity of the $[Nd_3(\mu_3\text{-}OH)_3(H_2O)_2]_n^{6n+}$ ribbon-like chain and the propionate groups.

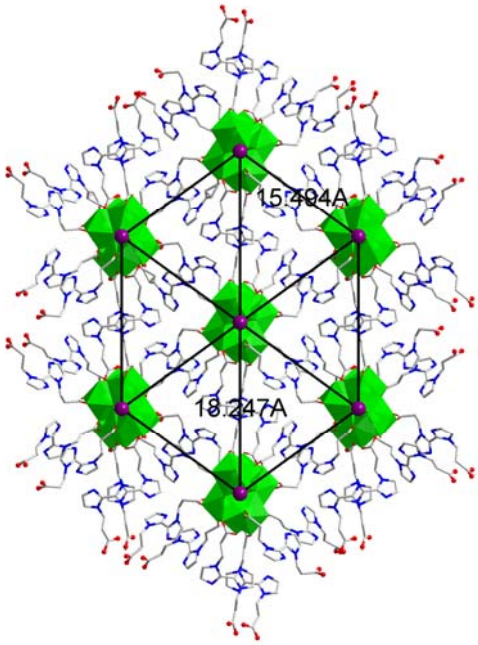

Fig. 5S 3-D open framework structure of **1** built of the $[Nd_3(\mu_3\text{-}OH)_3]_n^{6n+}$ ribbons interconnected by Pra_2biim^{2-}, showing the distances between two neighbouring ribbons.

Magnetic properties

The field-dependence of magnetization (M) of **1** is shown in Fig. 7S. M at 2K increases rapidly at low field and eventually reaches a plateau of 3.90 μ_B at 7T, which is markedly lower than the expected saturation value of 10.86 μ_B (3.62 μ_B for each Nd^{3+} ion[4]), indicating that spin orientations at even low lying excited states are dominated by the antiferromagnetic coupling with contributions from the crystal-field effect that eliminates the 3-fold degeneracy of the $^4I_{9/2}$ ground state of Nd^{3+}. M reaches the plateau value at markedly lower fields at the very slightly enhanced temperature (3K, 2.6 T; 4K, 1.8 T), in consistent with the much lower plateau value than the saturation value. The field-dependence of magnetization of **2** (Fig. 11S) behaves quite differently from that of **1** with the almost linear M−H plot. M reaches a maximum of 1.10 μ_B at 7T (2K), which is remarkably lower than the expected saturation value of 10.74 μ_B (3.58 μ_B for each Pr(III) ion[4]) as a consequence of both remarkable intra-chain antiferromagnetic coupling and spin-orbit effects. This value was more quickly achieved at slightly enhanced temperature (3K, 2.6 T; 4K, 1.6 T) as in the case of **1**. The M-H/T plots of both **1** and **2** at different temperatures show non-superposition, suggestive of the presence of magnetic anisotropy and/or low lying

excited states (Fig. 8S and 12S).

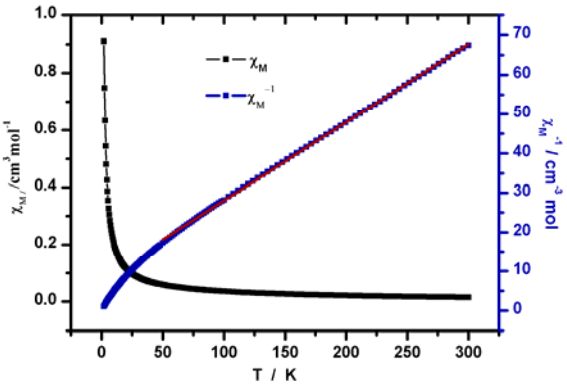

Fig. 6S Plots of temperature dependence of χ_M vs T and χ_M^{-1} vs T of **1**.

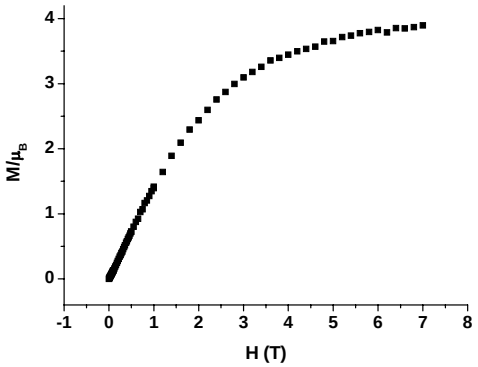

Fig. 7S *M* vs *H* plot of **1** at 2K.

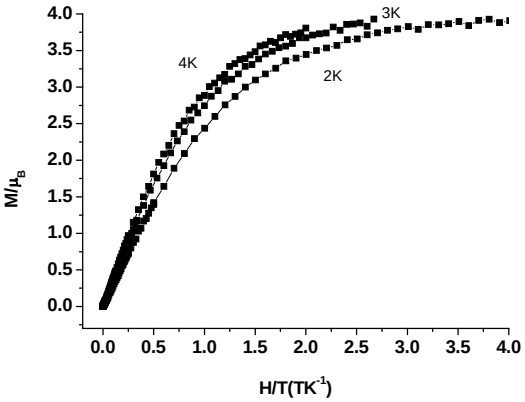

Fig. 8S *M* vs *H/T* plot of **1** at 2, 3 and 4K.

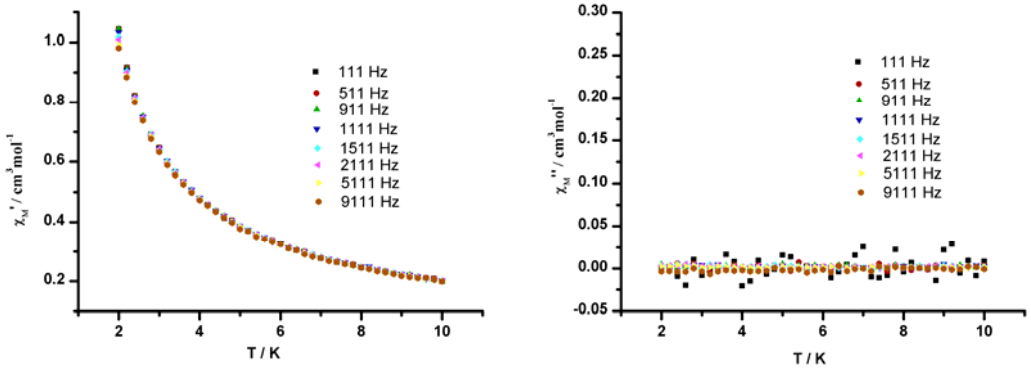

Fig. 9S Temperature dependence of ac susceptibilities for **1**.

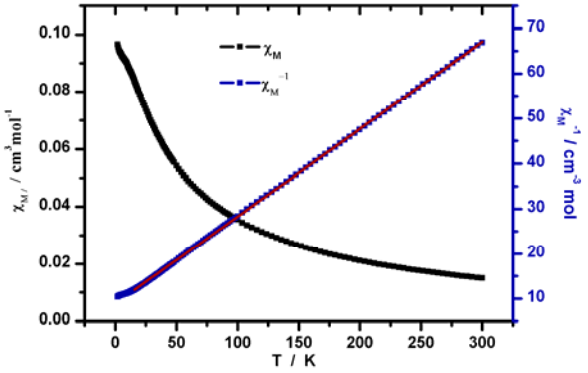

Fig. 10S Plots of temperature dependence of χ_M vs T and χ_M^{-1} vs T of **2**.

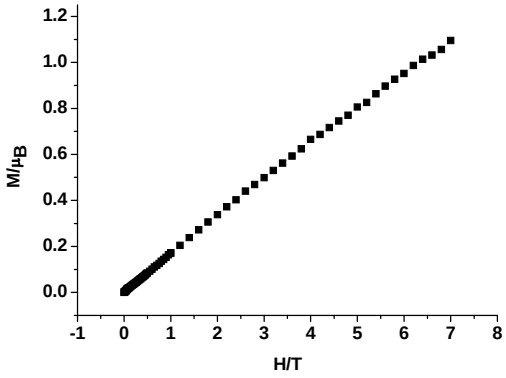

Fig. 11S *M* vs *H* plot of **2** at 2K.

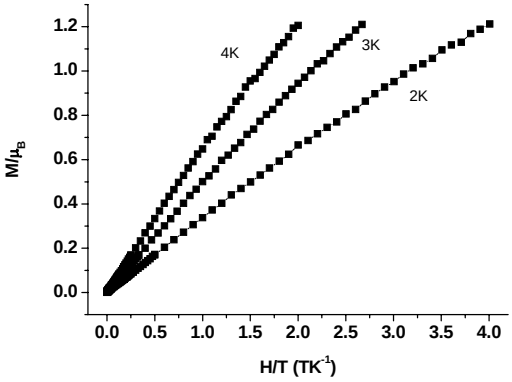

Fig. 12S *M* vs *H/T* plot of **2** at 2, 3 and 4K.

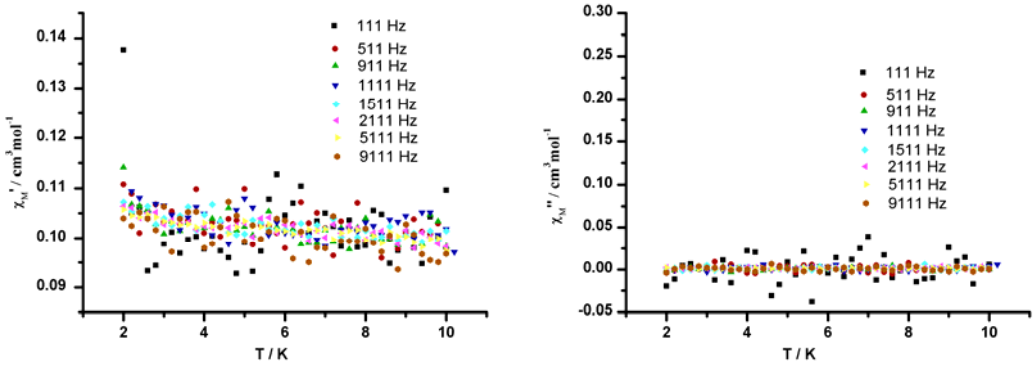

Fig. 13S Temperature dependence of ac susceptibilities for **2**.

Thermogravimetric analysis (TGA)

TGA study was performed in N_2 atomsophere at a heating rate of 10 °C min^{-1} from 40 to 1000 °C for compound **1**, **2** and **3**. As shown in Fig. 14S, the TGA diagram of **1** displays an initial the weight loss of 5.3 % between 40 and 135 °C, which correspond to the removal of 4 guest water molecules (calcd 5.1 %). Between 135 and 200 °C, **1**

shows the weight loss of 2.5 %, which correspond to the removal of 2 coordination aqua molecules (calcd 2.5 %). The TGA curve of **2** showed a weight loss of 5.2 % in the range of 40 – 130 °C, which could be attributed to the loss of 4 guest water molecules (calcd 5.1 %). The release of the coordination water molecules (2.4 %, expected 2.6%) took place between 130 and 190 °C. The TGA diagram of **3** revealed that the loss of 4 guest water molecules (5.5 %, calculated 5.1 %) occurred in the temperature range 40 – 125 °C. The release of the coordination water molecules (2.3 %, expected 2.6%) took place between 125 and 200 °C.

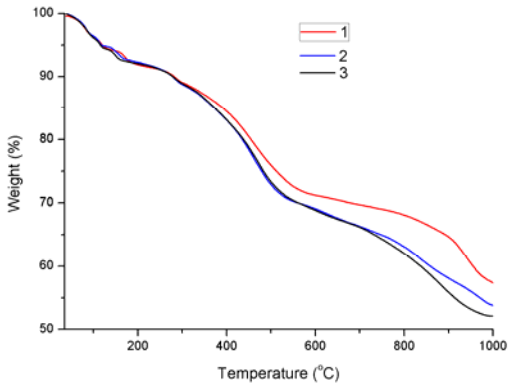

Fig. 14S TGA curves of compounds **1**-**3**.

Conformation analysis of the ligands

To understand the conformation of Pra_2biim^{2-} L1-L3 in compound **1**, the ligand conformation analysis is conducted as shown in Scheme 1S. The imidazole ring and C6 are coplanar, with the maxmium deviation from the least-squares plane less than 0.054 Å. The carboxylate group (C7, C8, O9 and O10) are also coplanar with the maximum deviation less than 0.062 Å. The conformation of Pra_2biim^{2-} is thus determined by the dihedral angle between the two imidazole rings and the three torsion angles C1-N5-C6-C7, N5-C6-C7-C8, and C6-C7-C8-O9 (or C6-C7-C8-O10), which, particularly the dihedral angles and C1-N5-C6-C7 torsion angle, also measure the extent to which the two propionate arms are repulsive to each other. As indicated in Table 5S and Figure 15S, Pra_2biim^{2-} displays *trans* configuration with the dihedral angles of 148.2(6), 139.5(4) and 125.7(5)°, respectively in L1, L2 and L3. It is notable that the two imidazole-propionate moieties are independent and have different conformation. The torsion angles of C1-N5-C6-C7/C1'-N5'-C6'-C7' are

-118.6(6)/145.0(6), -86.4(6)/146.5(5) and 109.6(7)/113.8(7)°, respectively in L1-L3, indicating that the two C6-C7 bond bend inside and outside, respectively in L1 and L2, and both outside in L3. The repulsion between the two bulky propionate arms (C6-C6', L1: 5.2563(8), L2: 5.0949(6), and L3: 4.9086(6) Å, C7-C7', L1: 7.7598(9), L2: 7.2340(7), and L3: 7.3665(5) Å). The dihedral angle of im-im and the repulsion between the two bulky propionate arms is larger than that found in these 3D helix-based Cd complexes due to the nitrogen atoms and oxygen atoms are coordinating to the metal atoms in Cd complexes.[3] The N5-C6-C7-C8 and C6-C7-C8-O9 torsion angles are presumably more directly determined by the coordination requirement of the propionate arms. One N5-C6-C7-C8 is clinal with the torsion angles of 117.5(4)°, the other of 173.1(4)° is coplanar and the carboxylate chains C6-C7-C8-O9 is coplanar with the torsion angles -177.9(4)/170.6(4)° of O9-C8-C7-C6 in L1. The N5-C6-C7-C8 is clinal with the torsion angles of -159.9(4)/82.8(6)°, and the carboxylate chains C6-C7-C8-O9 is also clinal with the torsion angles 136.1(4)/48.5(6)° of O9-C8-C7-C6 in L2. These values differ obviously from those found in L1 and L2 chains that feature the appropriately coplanar N5-C6-C7-C8 and C6-C7-C8-O9 in L3.

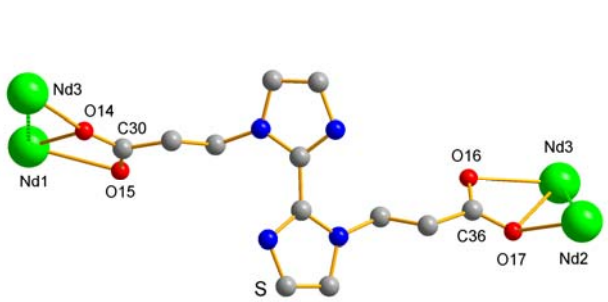

Mode I: μ5-η2:η1: η1:η1

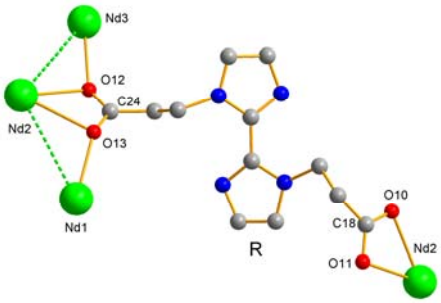

Mode II: μ4-η2:η2: η1:η1

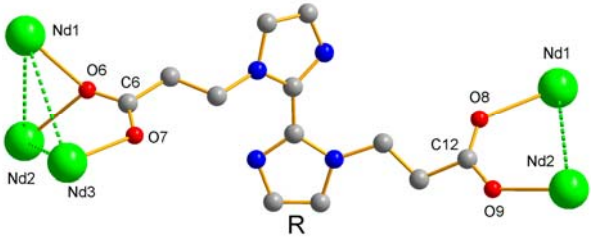

Mode III: μ4-η2:η1: η2:η1

Fig. 15S Coordination modes of three Pra_2biim^{2-} in **1**.

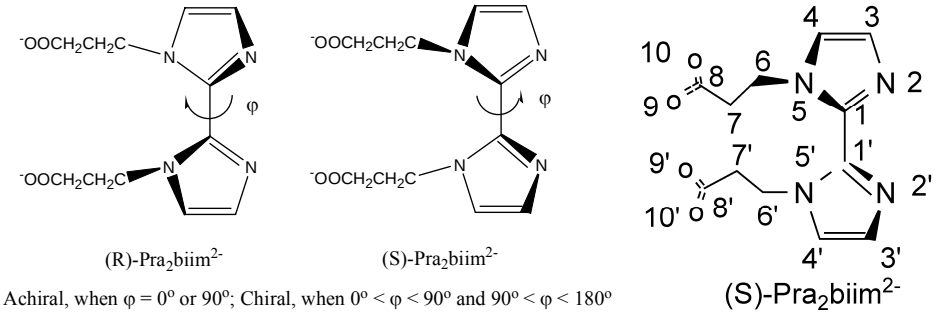

(R)-Pra_2biim^{2-} (S)-Pra_2biim^{2-}

Achiral, when $\varphi = 0^o$ or 90^o; Chiral, when $0^o < \varphi < 90^o$ and $90^o < \varphi < 180^o$

(S)-Pra_2biim^{2-}

Scheme 1S The configuration of Pra_2biim^{2-} (left) and S-Pra_2biim^{2-}, showing the number of atoms (right).

Table5S Comparison of the conformation of Pra_2biim^{2-} of complex **1** (°).

	Dihedral angle of im-im	Torsion angle of 1567 /1'5'6'7'	Torsion angle of 5678/5'6'7'8'	Torsion angle of 6789/6'7'8'9'
L1	148.2(6)	-118.6(6)/145.0(6)	117.5(4)/173.1(4)	-177.9(4)/170.6(4)
L2	139.5(4)	-86.4(6)/146.5(5)	-159.9(4)/82.8(6)	136.1(4)/48.5(6)
L3	125.7(5)	109.6(7)/113.8(7)	170.4(5)/174.8(5)	-158.0(5)/26.4(7)

Reference:

1 W. M. Barnett, R. G. Baughman, H. L. Collier, W. G. Vizuete, *J. Chem. Crystal.*, **1999**, *29*, 765.

2 G. M. Sheldrick, *Program for Crystal Structure Solution*, SHELXL-97, University of Gottingen, **1997.**

3 R. –L. Sang and L. Xu, CrystEngComm, 2010, 3579.

4 W. E. Hatfield, in *Solid State Chemistry: techniques* (Eds: A. K. Cheetham, P. Dav), Clarendon Press,Oxford, 1987, pp. 136.